

Work and heat distributions for a Brownian particle subjected to an oscillatory drive

Bappa Saha and Sutapa Mukherji

Department of Physics, Indian Institute of Technology, Kanpur-208 016

(Dated: June 13, 2021)

Using the Onsager-Machlup functional integral approach, we obtain the work distribution function and the distribution of the dissipated heat of a Brownian particle subjected to a confining harmonic potential and an oscillatory driving force. In the long time limit, the width of the work distribution function initially increases with the frequency of the driving force and finally saturates to a fixed value for large values of the angular frequency. Using the results from the work distribution part, we next obtain the distribution of the dissipated heat for the equilibrium initial condition. Using the method of steepest descent, we obtain a Gaussian distribution for small fluctuations in the large time limit. The distribution function, for a fixed time has been obtained numerically. It is shown that the heat distribution, in general, does not satisfy the transient fluctuation theorem.

I. INTRODUCTION

The fluctuation-dissipation theorem displaying the connection between the ‘friction coefficient’ and the fluctuations in thermodynamic variables has been derived for systems close to equilibrium [1, 2]. The role of fluctuations in nonequilibrium systems is described through a set of powerful, general results known as fluctuation theorems [3–11]. Fluctuation theorems have been proposed for various fluctuating thermodynamic quantities like heat, work, entropy production etc and they display the macroscopic irreversibility of the system subjected to nonequilibrium conditions. According to the fluctuation theorem, the probability $P(W_\tau = w\tau)$ that a time-integrated quantity $W_\tau = \int_0^\tau dt \dot{W}$ (W_τ may represent the work done by an external drive over time interval τ) has a value $w\tau$ satisfies the following relation

$$\lim_{\tau \rightarrow \infty} \frac{1}{\tau} \ln \frac{P(W_\tau = w\tau)}{P(W_\tau = -w\tau)} = w. \quad (1)$$

The asymmetry displayed in this equation is due to the external field responsible for driving the system out of equilibrium. Fluctuation theorems are of two kinds: the transient fluctuation theorem and the steady-state fluctuation theorem. In case of the transient fluctuation theorem, the system evolves from an initial equilibrium state at $\tau = 0$. For the steady-state fluctuation theorem, the system is in its nonequilibrium stationary state through out the entire time interval τ [3].

Onsager-Machlup used a functional integral approach in their original study on fluctuations in linear-relaxation processes [12, 13]. An outcome of a variational treatment on the functional integral is Onsager’s principle of minimum energy dissipation [14]. Since the development of the Onsager-Machlup fluctuation theory, there have been many efforts to extend their functional integral approach to systems far away from equilibrium [15–21]. Using the Onsager-Machlup approach for nonequilibrium steady states, Taniguchi and Cohen obtained the work and heat distribution functions of a Brownian particle dragged by a moving harmonic potential [18–20]. They showed the validity of the work fluctuation theorem in the long time limit for arbitrary initial conditions and discussed the extended heat fluctuation theorem for the heat distribution function. Similar methods have also been used to investigate the asymptotics of the work distribution functions for a number of nonequilibrium systems [22].

In the present work, we extend the Onsager-Machlup functional integral approach to obtain the distributions of the total work and the dissipated heat for a Brownian particle subjected to an external oscillatory driving force and a confining harmonic trap. We express the transition probability in a functional integral form in terms of a Lagrangian. The distribution of the total work done on the particle can be expressed in terms of an appropriate functional integral involving the transition probability. Our approach involves an explicit evaluation of the functional integral to obtain the general form of the distribution function. The distribution function reflects clearly the oscillatory features of the external drive. In the long time limit, the work distribution function becomes Gaussian with a variance that depends non-trivially on the angular frequency of the oscillatory drive. Analytical results appear to be in agreement with those from numerical simulations. Results from the work distribution part are used further to obtain the Fourier transform of the distribution of the dissipated heat. Using the method of steepest descent, we have obtained a Gaussian distribution for the dissipated heat over the central region (small fluctuations). The general behavior of the heat distribution, at a fixed time (not necessarily large), is obtained by numerically evaluating the inverse Fourier transform. The numerically evaluated distribution for a finite time and the simulation results show that the distribution, in general, does not satisfy the transient fluctuation theorem.

Much before the application of the Onsager-Machlup theory to the nonequilibrium stationary state problems involving a dragged Brownian particle [18, 19], it has been shown in a general way that the work distribution function

for a parabolic potential with an arbitrary motion of the center satisfies the transient and stationary state fluctuation theorem [8, 23]. The distribution function of heat for a Brownian particle dragged by a moving parabolic potential has been studied in [9, 18, 19, 24]. The present work provides a detailed evaluation of the work distribution and the distribution of the dissipated heat for a nonequilibrium oscillatory state using the Onsager-Machlup path integral approach. Using this method, the work distribution for an oscillatory potential has been obtained earlier in [25]. The work distribution in [25] is essentially for the mechanical part of the work associated with the driving force. On the other hand, the work distribution evaluated here is for the total work which consists of the change in the potential energy as well as the dissipative part. We have further used this result to find the distribution of the dissipated heat. We obtain the Fourier transform of the heat distribution whose Fourier inverse is found out using the method of steepest descent under certain conditions and also through a direct numerical integration. We also independently obtain the heat distribution function through numerical simulations. The numerical integration and the simulation results indicate, in general, a non-Gaussian nature of the heat distribution function.

The paper is organized in the following way. In section II, we introduce the Langevin equation describing the motion of the Brownian particle. Deriving the Fokker-Planck equation, we then obtain a functional integral description for the transition probability. In section III, the explicit form of the transition probability is determined using a variational approach. The functional integral description of the transition probability involves an Onsager-Machlup type Lagrangian which is used later in section IV, to obtain the entropy production rate for this system. The energy-conservation principle further allows us to identify the total work done, the rate of mechanical work, that contributes to the potential energy, and the dissipative part of the work [8]. In section V, we obtain a general expression for the distribution function of the total work. Section VI provides a derivation of the distribution of the dissipated heat. The details on the numerical simulations of our system are provided in section VII. We summarize our work in Section VIII. Some of the details of the calculations related to the derivation of the transition probability, and the distributions are presented in appendices.

II. BROWNIAN PARTICLE IN PRESENCE OF AN OSCILLATORY DRIVING FORCE

The over-damped Langevin equation describing the motion of the Brownian particle is given by

$$\alpha \frac{dx_t}{dt} = -\Xi \cos \omega t - kx_t + \zeta_t, \quad (2)$$

where α is the friction coefficient and ζ_t is a Gaussian distributed noise arising due to the coupling of the system with a thermal reservoir. The noise distribution is specified through the averages $\langle \zeta_t \rangle = 0$ and $\langle \zeta_{t_1} \zeta_{t_2} \rangle = g \delta(t_1 - t_2)$, with g being the strength of the noise. The particle is subjected to a confining harmonic potential $\frac{k}{2}x_t^2$ and an oscillatory force of strength Ξ .

Our aim here is to find out the transition probability $P(x_f, t_f | x_i, t_i)$ which describes the probability of finding the Brownian particle at position x_f at time t_f given that the particle is located at x_i at time t_i . In order to determine this, we obtain the Fokker-Planck equation for the probability distribution function $\rho(x, t)$ of finding the particle at x at time t . The Fokker-Planck equation is

$$\frac{\partial \rho(x, t)}{\partial t} = \mathcal{L} \rho(x, t), \quad (3)$$

where the Fokker-Planck operator \mathcal{L} is

$$\mathcal{L} = \frac{\partial}{\partial x} \left[\left(\frac{kx}{\alpha} + \frac{\Xi}{\alpha} \cos \omega t \right) + \frac{g}{2\alpha^2} \frac{\partial}{\partial x} \right]. \quad (4)$$

From now onwards, we use the following parameters $D = \frac{g}{2\alpha^2}$, $\gamma = \frac{k}{\alpha}$ and $\eta = \frac{\Xi}{\alpha}$. The expression of D can be further simplified by using the fluctuation-dissipation theorem [2] that leads to $g = 2\alpha/\beta$ and $D = 1/(\alpha\beta)$. The Fokker-Planck equation allows us to obtain the following functional integral description for the transition probability $P(x_f, t_f | x_i, t_i)$ [26, 27]

$$P(x_f, t_f | x_i, t_i) = \int_{x_i}^{x_f} \mathcal{D}x_t \exp \left[\int_{t_i}^{t_f} dt L(x_t, \dot{x}_t, t) \right], \quad (5)$$

where

$$L(x_t, \dot{x}_t, t) = -\frac{1}{4D} (\gamma x_t + \dot{x}_t + \eta \cos \omega t)^2. \quad (6)$$

Here $\int_{x_i}^{x_f} \mathcal{D}x_t$ denotes a sum over all possible paths between the initial and final points, x_i and x_f , respectively.

In

$$\exp \left[-\frac{1}{4D} \int_{t_i}^{t_f} dt (\gamma x_t + \dot{x}_t + \eta \cos \omega t)^2 \right] \quad (7)$$

the integrand as well as the integral are either zero or positive. The condition for zero of the integrand is satisfied by the average path which, from equation (2), is the solution of

$$\frac{d\langle x_t \rangle}{dt} = -\eta \cos \omega t - \gamma \langle x_t \rangle. \quad (8)$$

It is equivalent to saying that at each time instant, one considers the average position of the Brownian particle. The path constructed this way is the average path. There is another special path which corresponds to a path in a given time interval $[t_i : t_f]$ with maximum probability. This path is the most probable path that contributes maximally to the transition probability [28].

III. TRANSITION PROBABILITY

The most probable path for the Brownian particle can be found out by extremizing the integral $\int_{t_i}^{t_f} dt L(x_t, \dot{x}_t, t)$ in equation (5). The extremization leads to the Euler-Lagrange equation

$$\frac{d}{dt} \left(\frac{\partial L}{\partial \dot{x}_t} \right) - \frac{\partial L}{\partial x_t} = 0, \quad (9)$$

from which we find the following equation for the most probable path

$$\ddot{x}_t - \gamma^2 x_t - \eta(\omega \sin \omega t + \gamma \cos \omega t) = 0, \quad (10)$$

where an overdot denotes a derivative with respect to time. The most probable path denoted as \tilde{x}_t is found as

$$\tilde{x}_t = A \exp[\gamma t] + B \exp[-\gamma t] - \frac{\eta\gamma}{\omega^2 + \gamma^2} \cos \omega t - \frac{\eta\omega}{\omega^2 + \gamma^2} \sin \omega t, \quad (11)$$

where A and B are the integration constants which depend on the initial conditions. Using the initial conditions, $\tilde{x}_t = x_i$ at $t = t_i = 0$ and $\tilde{x}_t = x_f$ at $t = t_f$, we find

$$A = x_i + \frac{\gamma\eta}{\omega^2 + \gamma^2} - \frac{1}{e^{-\gamma t_f} - e^{\gamma t_f}} \left[e^{\gamma t_f} \left(-\frac{\eta\gamma}{\omega^2 + \gamma^2} - x_i \right) + \frac{\eta\omega}{\omega^2 + \gamma^2} \sin \omega t_f + \frac{\eta\gamma}{\omega^2 + \gamma^2} \cos \omega t_f + x_f \right], \quad (12)$$

$$B = x_i + \frac{\eta\gamma}{\omega^2 + \gamma^2} - A. \quad (13)$$

The corresponding Lagrangian for the most probable path is given by $L(\tilde{x}_t, \dot{\tilde{x}}_t, t) = -\frac{1}{4D}(4\gamma^2 A^2 \exp[2\gamma t])$.

In order to obtain the explicit form of $P(x_f, t_f | x_i, t_i)$, we need to do the functional integration in (5). The functional integration is done by considering paths with infinitesimal deviations, z_t , about the most probable path as $x_t = \tilde{x}_t + z_t$ and $\dot{x}_t = \dot{\tilde{x}}_t + \dot{z}_t$. Expanding in small z_t and \dot{z}_t , we have

$$\begin{aligned} & \int_{t_i}^{t_f} dt L(\tilde{x}_t + z_t, \dot{\tilde{x}}_t + \dot{z}_t, t) \\ &= \int_{t_i}^{t_f} dt L(\tilde{x}_t, \dot{\tilde{x}}_t, t) + \int_{t_i}^{t_f} dt \left[\frac{\partial L(\tilde{x}_t, \dot{\tilde{x}}_t, t)}{\partial \tilde{x}_t} - \frac{d}{dt} \frac{\partial L(\tilde{x}_t, \dot{\tilde{x}}_t, t)}{\partial \dot{\tilde{x}}_t} \right] z_t - \frac{1}{4D} \int_{t_i}^{t_f} dt \left[\gamma^2 z_t^2 + \dot{z}_t^2 + 2\gamma z_t \dot{z}_t \right]. \end{aligned} \quad (14)$$

The term with a negative sign in the second integral in expression (14) is obtained after doing an integration by parts of $\int_{t_i}^{t_f} dt \frac{\partial L}{\partial \dot{\tilde{x}}_t}(\tilde{x}_t, \dot{\tilde{x}}_t) \dot{z}_t$ that appears at the first order in the expansion. The transition probability can now be expressed as

$$P(x_f, t_f | x_i, t_i) = \exp \left[\int_{t_i}^{t_f} dt L(\tilde{x}_t, \dot{\tilde{x}}_t, t) \right] \int \mathcal{D}z \exp \left[-\frac{1}{4D} \int_{t_i}^{t_f} dt \left[\gamma^2 z_t^2 + \dot{z}_t^2 + 2\gamma z_t \dot{z}_t \right] \right]. \quad (15)$$

The functional integral in the above expression is to be done with the constraints $z_{t_i} = z_{t_f} = 0$. Appendix A provides the details of calculation of the functional integral in equation (15). The final result for the transition probability is

$$P(x_f, t_f | x_i, t_i) = \left(\frac{2\pi D}{\gamma} \right)^{-1/2} \exp \left[-\frac{\gamma A^2}{2D} (e^{2\gamma t_f} - e^{2\gamma t_i}) \right] \left(1 - \exp[-2\gamma(t_f - t_i)] \right)^{-1/2}. \quad (16)$$

Clearly, at large time $t_f \rightarrow \infty$, $A \approx (x_f + \frac{\eta\omega}{\omega^2 + \gamma^2} \sin \omega t_f + \frac{\eta\gamma}{\omega^2 + \gamma^2} \cos \omega t_f) e^{-\gamma t_f}$. In this limit, the transition probability has the form,

$$P(x_f, t_f | x_i, t_i) = \left(\frac{2\pi D}{\gamma} \right)^{-1/2} \exp \left[-\frac{\gamma}{2D} \left(x_f + \frac{\eta\omega}{\omega^2 + \gamma^2} \sin \omega t_f + \frac{\eta\gamma}{\omega^2 + \gamma^2} \cos \omega t_f \right)^2 \right]. \quad (17)$$

The above result implies that in the absence of the oscillatory force ($\eta = 0$), one recovers, at large time, the equilibrium probability distribution

$$\begin{aligned} \rho_{\text{eq}}(x_f) &= \int dx_i P(x_f, t_f | x_i, t_i) f(x_i, t_i) \approx \left(\frac{2\pi D}{\gamma} \right)^{-1/2} \exp \left[-\frac{\gamma x_f^2}{2D} \right] \\ &= \left(\frac{2\pi}{k\beta} \right)^{-1/2} \exp \left[-\beta(kx_f^2/2) \right], \end{aligned} \quad (18)$$

where we have assumed the initial distribution, $f(x_i, t_i)$, to be normalized, i.e., $\int f(x_i, t_i) dx_i = 1$.

IV. ENERGY CONSERVATION AND ONSAGER-MACHLUP LAGRANGIAN

In section II, we have shown that the transition probability can be expressed as a functional integral involving an Onsager-Machlup type Lagrangian. The purpose of this section is to use Langevin equation to obtain a formal expression for the work done by the external force. The Onsager-Machlup Lagrangian may be used to identify the rate of entropy production in this process. We show that the expressions for the work done by the external force and the entropy production rate, as obtained here, consistently satisfy the energy conservation principle.

The Langevin equation expresses the force-balance condition,

$$\left(-\alpha \frac{dx}{dt} + \zeta \right) - \Xi \cos \omega t - kx = 0, \quad (19)$$

where terms in the bracket represent the force on the particle due to the reservoir. For simplicity, in this subsection, we have removed the subscript of the variable x . Multiplying with a small displacement of the particle, this equation can be converted to the energy conservation equation

$$d\mathcal{Q} + dU = dW, \quad (20)$$

where $dU = \frac{\partial U(x,t)}{\partial x} dx + \frac{\partial U(x,t)}{\partial t} dt$ is an exact differential with $U(x,t) = \Xi x \cos \omega t + \frac{1}{2} kx^2$ as the potential energy and $dW = \frac{\partial U(x,t)}{\partial t} dt$ is the work done by the external force [29]. The term $d\mathcal{Q} = -(-\alpha \frac{dx}{dt} + \zeta) dx$ is the heat released by the particle to the heat reservoir. This work W , referred to in this paper as the total work, thus consists of a dissipative part associated with the heat release and a mechanical part associated with the change in U . Over the interval $\{t_i : t_f\}$, various quantities can be written as

$$\Delta \mathcal{Q} = T \int_{t_i}^{t_f} \dot{S} dt, \quad (21)$$

$$\Delta W = \int_{t_i}^{t_f} \dot{W} dt = -\Xi \omega \int_{t_i}^{t_f} dt x \sin \omega t, \quad (22)$$

$$\Delta U = \int_{t_i}^{t_f} dU = \left(\frac{1}{2} kx^2 + \Xi x \cos \omega t \right) \Big|_{t_i}^{t_f}, \quad (23)$$

where $\dot{W} = -\Xi x \omega \sin \omega t$.

The Onsager-Machlup Lagrangian can be expressed as

$$\begin{aligned} L &= -\frac{1}{2k_B} \left\{ [\gamma^2 x^2 + 2\gamma\eta x \cos \omega t] + [\dot{x}^2 + \eta^2 (\cos \omega t)^2] - [-2\gamma x \dot{x} - 2\eta \dot{x} \cos \omega t] \right\} \frac{\alpha}{2T} \\ &= -\frac{1}{2k_B} \left\{ \Phi(\dot{x}, t) + \Psi(x, t) - \dot{S}(x, \dot{x}, t) \right\}, \end{aligned} \quad (24)$$

where

$$\Phi(\dot{x}, t) = \frac{\alpha}{2T} (\dot{x}^2 + \eta^2 (\cos \omega t)^2), \quad (25)$$

$$\Psi(x, t) = \frac{\alpha}{2T} (\gamma^2 x^2 + 2\gamma\eta x \cos \omega t) \quad (26)$$

are the dissipation functions and

$$\dot{S}(x, \dot{x}, t) = -2 \left(\frac{k}{\alpha} \right) x \dot{x} \frac{\alpha}{2T} - 2 \left(\frac{\Xi}{\alpha} \right) \left(\frac{\alpha}{2T} \right) \dot{x} \cos \omega t \quad (27)$$

is the rate of entropy production. Using (27), (21) and (22), one finds the change in the energy as expressed in (23).

V. WORK DISTRIBUTION

We now determine the work distribution $P(W, t) = \langle \langle \delta(W - \mathcal{W}(\{x_t\})) \rangle \rangle$, where $\mathcal{W}(\{x_t\}) = \int_{t_i}^{t_f} dt \frac{\partial U(x_t, t)}{\partial t}$ denotes the work done by the time-dependent oscillatory force along the path x_t in time interval $[t_i : t_f]$ and $P(W, t)$ implies the probability that this work has a value W . $\langle \langle - \rangle \rangle$ denotes a functional average over all possible paths in the given time interval and integrals over initial and final positions.

We express $P(W)$ in terms of the Fourier transform of $\mathcal{W}(\{x_t\})$ as

$$P(W) = \frac{1}{2\pi} \int_{-\infty}^{\infty} d\lambda e^{i\lambda W} \langle \langle e^{-i\lambda \mathcal{W}(\{x_t\})} \rangle \rangle. \quad (28)$$

The functional integral can be expressed in terms of the transition probability shown in (5). Since the Lagrangian function L in the transition probability has a prefactor β , it is convenient if we introduce a β in equation (28) and re-express it as,

$$P(W) = \frac{\beta}{2\pi} \int_{-\infty}^{\infty} d\lambda e^{i\lambda \beta W} \langle \langle e^{-i\lambda \beta \mathcal{W}(\{x_t\})} \rangle \rangle. \quad (29)$$

Thus

$$\begin{aligned} \langle \langle e^{-i\lambda \beta \mathcal{W}(\{x_t\})} \rangle \rangle &= \int dx_f \int dx_i f(x_i, t_i) \int_{x_i}^{x_f} \mathcal{D}x_t e^{-i\lambda \beta \mathcal{W}(\{x_t\})} e^{\int_{t_i}^{t_f} dt L(x_t, \dot{x}_t, t)} \\ &= \int dx_f \int dx_i f(x_i, t_i) \mathcal{F}(x_f, x_i, \lambda), \end{aligned} \quad (30)$$

where

$$\mathcal{F}(x_f, x_i, \lambda) = \int_{x_i}^{x_f} \mathcal{D}x_t e^{\int_{t_i}^{t_f} dt \left[L(x_t, \dot{x}_t, t) - i\lambda \beta \dot{\mathcal{W}}(x_t) \right]}. \quad (31)$$

Here the functional average is done over all possible paths extending from x_i to x_f over the time interval $[t_i : t_f]$. The final result is obtained upon averaging over all initial points with the distribution $f(x_i, t_i)$ and integrating over the final point. As discussed before, in our case $\dot{\mathcal{W}}(x_t) = \frac{\partial U}{\partial t} = -\Xi x_t \omega \sin(\omega t)$. The functional integral in (31) is evaluated by maximizing the integral $\int_{t_i}^{t_f} dt \left[L(x_t, \dot{x}_t, t) - i\lambda \beta \dot{\mathcal{W}}(x_t) \right]$. This leads to the Euler-Lagrange equation

$$\frac{d}{dt} \left(\frac{\partial L(x_t, \dot{x}_t, t)}{\partial \dot{x}_t} \right) - \frac{\partial L(x_t, \dot{x}_t, t)}{\partial x_t} + i\lambda \beta \frac{\partial \dot{\mathcal{W}}(x_t)}{\partial x_t} = 0. \quad (32)$$

The Euler-Lagrange equation written in terms of x_t ,

$$\ddot{x}_t - \gamma^2 x_t - (\eta\omega - i(2D\lambda \beta \Xi \omega)) \sin \omega t - \eta\gamma \cos \omega t = 0 \quad (33)$$

has a solution of the form

$$x_t^* = A_W e^{\gamma t} + B_W e^{-\gamma t} - \frac{(\eta\omega - i\bar{\lambda})}{\omega^2 + \gamma^2} \sin \omega t - \frac{\eta\gamma}{\omega^2 + \gamma^2} \cos \omega t, \quad (34)$$

where $\bar{\lambda} = 2D\lambda\beta\Xi\omega = 2\lambda\eta\omega$. The two integration constants, A_W and B_W , determined using the initial and final conditions, $x_t^* = x_f$, at $t = t_f$ and $x_t^* = x_i$ at $t = t_i = 0$, are

$$A_W = \left[x_f - \left(x_i + \frac{\eta\gamma}{(\omega^2 + \gamma^2)} \right) e^{-\gamma t_f} + \frac{\eta(\omega \sin \omega t_f + \gamma \cos \omega t_f)}{\omega^2 + \gamma^2} - \frac{i\bar{\lambda} \sin \omega t_f}{\omega^2 + \gamma^2} \right] (\exp[\gamma t_f] - \exp[-\gamma t_f])^{-1} \quad (35)$$

$$\text{and } B_W = x_i + \frac{\eta\gamma}{\gamma^2 + \omega^2} - A_W. \quad (36)$$

The quantity $L(x_t^*, \dot{x}_t^*) - i\lambda\beta\dot{W}(x_t^*)$ now has a form

$$L(x_t^*, \dot{x}_t^*) - i\lambda\beta\dot{W}(x_t^*) = -\frac{1}{4D} \left[2\gamma A_W e^{\gamma t} + \frac{i\bar{\lambda}}{(\omega^2 + \gamma^2)} (\gamma \sin \omega t + \omega \cos \omega t) \right]^2 + \frac{i\bar{\lambda}}{2D} x_t^* \sin \omega t. \quad (37)$$

As before, the evaluation of $\mathcal{F}(x_f, x_i, \lambda)$ is done about the path (x_t^*, \dot{x}_t^*) which maximizes $\int_{t_i}^{t_f} dt \left[L(x_t, \dot{x}_t, t) - i\beta\lambda\dot{W}(x_t) \right]$. Thus

$$\mathcal{F}(x_i, x_f, \lambda) = e^{\int_{t_i}^{t_f} dt [L(x_t^*, \dot{x}_t^*) - i\lambda\beta\dot{W}(x_t^*)]} \int \mathcal{D}z_t e^{-\frac{1}{4D} \int_{t_i}^{t_f} dt (\gamma z_t + \dot{z}_t)^2}, \quad (38)$$

where z_t describes a small deviation about the maximal path as $x_t = x_t^* + z_t$ and $\dot{x}_t = \dot{x}_t^* + \dot{z}_t$ with the condition that z_t vanishes at the initial and final time points. The derivation of equation (38) is similar to that done before for the transition probability. The functional integral $\int \mathcal{D}z_t e^{-\frac{1}{4D} \int_{t_i}^{t_f} dt (\gamma z_t + \dot{z}_t)^2}$ has been evaluated earlier (see Appendix A). Using this result, we find

$$\mathcal{F}(x_f, x_i, \lambda) = \left(\frac{2\pi D}{\gamma} \right)^{-1/2} (1 - e^{-2\gamma t_f})^{-1/2} e^{-\frac{1}{4D} (x_f^2 c_1 + x_f c_2 + c_3)}. \quad (39)$$

The expressions for c_1, c_2, c_3 are given in Appendix B.

Combining equations (29) and (30), we may write

$$P(W) = \frac{\beta}{2\pi} \int dx_i f(x_i, t_i) \int_{-\infty}^{\infty} d\lambda e^{i\lambda\beta W} \int_{-\infty}^{\infty} dx_f \mathcal{F}(x_f, x_i, \lambda). \quad (40)$$

Using (39), and doing a Gaussian integration over x_f , we obtain

$$P(W) = \left(\frac{2\gamma}{c_1} \right)^{1/2} (1 - e^{-2\gamma t_f})^{-1/2} \frac{1}{2\eta\omega} \left(\frac{\beta}{2\pi} \right) \int dx_i f(x_i, t_i) \int_{-\infty}^{\infty} d\bar{\lambda} e^{-(m_2 \bar{\lambda}^2 + m_1 \bar{\lambda})} e^{i\bar{\lambda} W}, \quad (41)$$

where $\bar{W} = \frac{W}{2D\beta\Xi\omega}$. The expressions for m_1 and m_2 are also given in Appendix B.

After completing the integration over $\bar{\lambda}$, we have

$$P(W) = \left(\frac{\gamma\beta^2}{2\pi c_1 m_2} \right)^{1/2} \frac{(1 - e^{-2\gamma t_f})^{-1/2}}{2\eta\omega} \int dx_i f(x_i, t_i) \exp \left[-\frac{(\bar{W} - W_m)^2}{4m_2} \right], \quad (42)$$

where $W_m = m_1/i$.

In the large time limit ($t_f \rightarrow \infty$), the distribution function (42) becomes independent of the initial distribution $f(x_i, t_i)$ ($\int dx_i f(x_i, t_i) = 1$). In this limit, the work distribution has the form

$$\lim_{t_f \rightarrow \infty} P(W, t_f) \sim \frac{\beta}{2\eta\omega} \frac{1}{(2\pi\sigma^2)^{1/2}} \exp \left[-\frac{(\bar{W} - \eta\omega\sigma^2)^2}{2\sigma^2} \right], \quad (43)$$

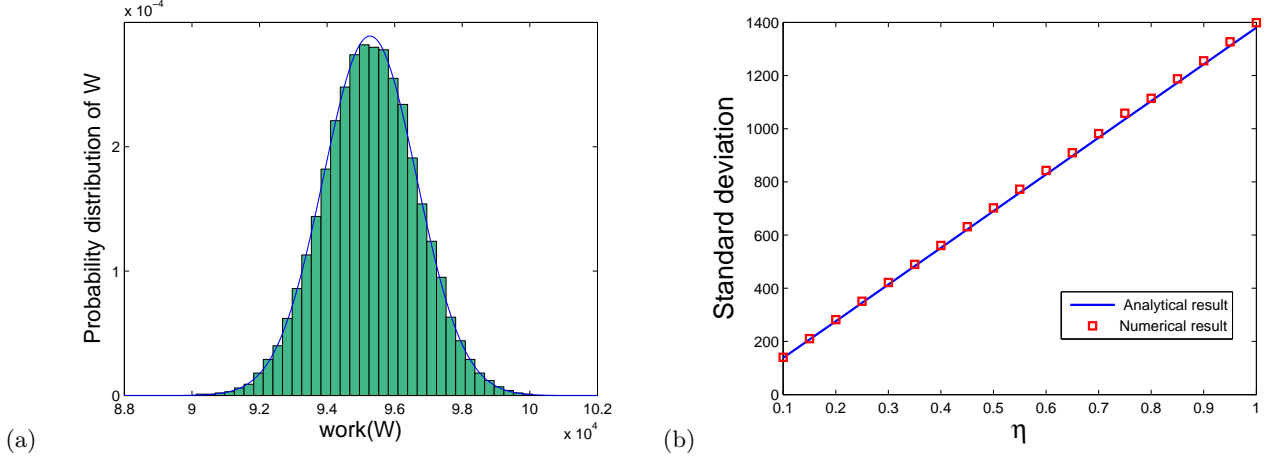


FIG. 1: (a) Work distribution at large time $t_f = 1000$. The solid blue curve is the plot of the analytical result given by equation(43). The parameter values are $D = 0.05, \omega = 0.1\pi, \gamma = 0.07, \beta = 0.1, \alpha = 200, \eta = 1$. The histogram is obtained from numerical simulations, where, the final displacement and the work values are computed for 40000 number of realizations with time-step, $\Delta t = 0.05$. (b) Variation of the width of the work distribution with the strength of the oscillatory force η . The work values are calculated for final time $t_f = 1000$. The solid blue line represents the standard deviation given by equation (45) and the red squares correspond to the numerical results. The other parameter values are $D = 0.05, \omega = 0.1\pi, \gamma = 0.07, \beta = 0.1, \alpha = 200$. The small time interval is $\Delta t = 0.25$. For each η , the work values are computed for 30000 realizations.

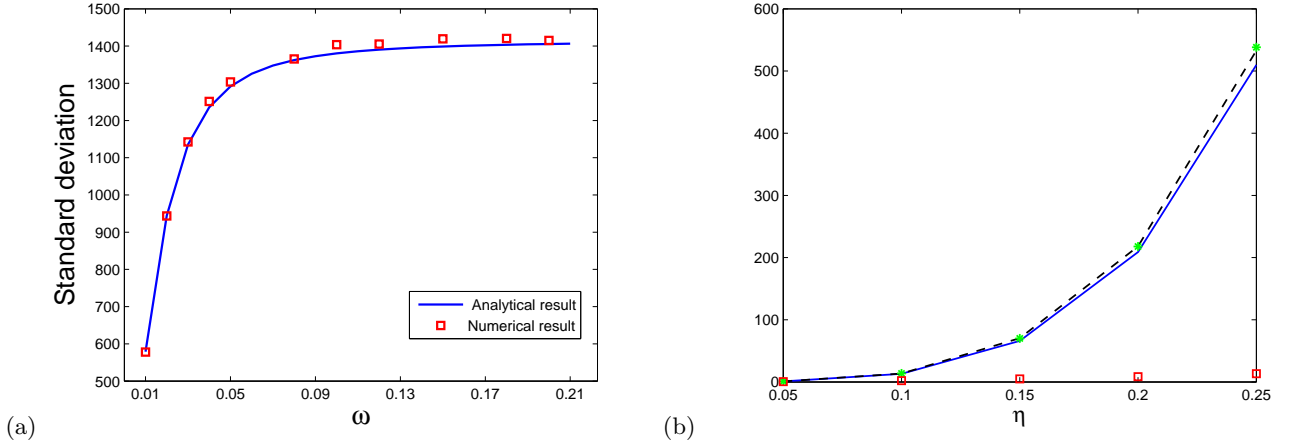


FIG. 2: (a) Variation of the width of the work distribution with the angular frequency ω (in the unit of π) of the oscillatory force at large time $t_f = 1000$. The solid blue curve corresponds to the analytical value of the standard deviation given by equation (45) and the red squares correspond to numerical results. The other parameter values are $D = 0.05, \gamma = 0.07, \beta = 0.1, \alpha = 200, \eta = 1$. The small time interval is $\Delta t = 0.08$. For each ω , the work-values have been computed for 30000 realizations. (b) Plot of the variance and the central fourth moment of the work distribution with the strength, η , of the oscillatory force at time $t_f = 1000$. The solid blue line is obtained from equation(46) and the black dashed line is the numerical value of $3(\langle W^2 \rangle - \langle W \rangle^2)^2$. The green stars and the red squares are the simulation results of $\langle (W - \langle W \rangle)^4 \rangle$ and $(\langle W^2 \rangle - \langle W \rangle^2)$, respectively. The other parameter values are $D = 0.01, \omega = 0.05\pi, \gamma = 0.07, \beta = 20, \Delta t = 0.2$. All data are obtained after averaging over 50000 realizations.

where $\sigma^2 = \frac{t_f}{4D(\omega^2 + \gamma^2)}$. A similar Gaussian distribution in the long time limit was found for a dragged Brownian particle in [18, 23, 30]. Thus, in the long time ($t_f \rightarrow \infty$) limit, the work distribution function satisfies the work fluctuation theorem,

$$\lim_{t_f \rightarrow \infty} \frac{P(W, t_f)}{P(-W, t_f)} = \exp[\beta W] \quad (44)$$

for any initial condition.

In the present problem of a nonequilibrium oscillatory state, the width of the distribution

$$\langle (W^2) - \langle W \rangle^2 \rangle^{1/2} = \frac{2\eta\omega\sigma}{\beta} \quad (45)$$

increases linearly with the strength of the oscillatory force. Further, for a given strength of the oscillatory force, the width increases initially with the angular frequency ω and finally saturates to a value that depends on the strength of the oscillatory drive. The fourth central moment of the work distribution in equation (43) is

$$\langle (W - \langle W \rangle)^4 \rangle = \frac{48\eta^4\omega^4\sigma^4}{\beta^4}. \quad (46)$$

In the following section, we derive the distribution of heat using the results obtained so far.

VI. DISTRIBUTION OF DISSIPATED HEAT

The dissipated heat can be defined as

$$Q = \mathcal{W}(x_t) - \Delta U, \quad (47)$$

where $\Delta U = U(x_f, t_f) - U(x_i, t_i)$ and $U = \frac{1}{2}kx^2 + \Xi x \cos(\omega t)$. The distribution of heat can be expressed as

$$P(Q) = \frac{\beta}{2\pi} \int_{-\infty}^{\infty} d\lambda e^{i\lambda\beta Q} \langle \langle e^{-i\lambda\beta Q} \rangle \rangle. \quad (48)$$

We denote $\langle \langle e^{-i\lambda\beta Q} \rangle \rangle$ by $P(i\lambda Q, t_f)$ and it can be determined by evaluating the functional averages over all possible paths as well as the integrals over initial and final positions. Hence,

$$P(i\lambda Q, t_f) = \int dx_f \int dx_i f(x_i, t_i) e^{i\lambda\beta(U(x_f, t_f) - U(x_i, t_i))} \mathcal{F}(x_f, x_i, \lambda), \quad (49)$$

where, we directly substitute the expression of $\mathcal{F}(x_f, x_i, \lambda)$ from equation(39).

Assuming that the system evolves from initial equilibrium distribution, we express the normalized initial distribution of position $f(x_i, t_i = 0)$ as

$$f(x_i) = \sqrt{\frac{\gamma}{2\pi D}} e^{-\frac{\eta^2}{2D\gamma}} e^{-(\frac{1}{2}\gamma x_i^2 + \eta x_i)/D}. \quad (50)$$

The shifted Gaussian nature of the distribution follows from the confining harmonic potential (defined after equation (20)) with its minimum varying in an oscillatory fashion. After performing the integrations over x_f and x_i , we write the final form of $P(i\lambda Q, t_f)$ as a function of λ ,

$$P(i\lambda Q, t_f) = \frac{e^{-\eta^2/(2D\gamma)}}{(1 + \lambda^2 - e^{-2\gamma t_f} \lambda^2)^{1/2}} \exp(q_n/q_d), \quad (51)$$

where, q_d and q_n are given by,

$$q_d = 4D\gamma e^{2\gamma t_f} (1 + \lambda^2 - e^{-2\gamma t_f} \lambda^2) (\omega^2 + \gamma^2)^2 \quad (52)$$

and

$$q_n = l_4\lambda^4 + il_3\lambda^3 + l_2\lambda^2 + il_1\lambda + l_0, \quad (53)$$

where the expressions for l_4, l_3, l_2, l_1 and l_0 are given in Appendix B. Substituting equation(51) into (48), we have

$$P(Q) = \frac{\beta}{2\pi} \int_{-\infty}^{\infty} d\lambda e^{i\lambda\beta Q} \frac{e^{-\eta^2/(2D\gamma)}}{(1 + \lambda^2 - e^{-2\gamma t_f} \lambda^2)^{1/2}} \exp(q_n/q_d). \quad (54)$$

In order to obtain an approximate form of the distribution in the $t_f \rightarrow \infty$ limit, equation (54) can be written as,

$$P(Q) = \frac{\beta}{2\pi} e^{-\frac{\eta^2}{2D\gamma}} \int_{-\infty}^{\infty} \frac{\exp(t_f S(\lambda))}{(1 + \lambda^2)^{1/2}} d\lambda. \quad (55)$$

where,

$$S(\lambda) = i\lambda\beta Q_f - \frac{\omega^2\eta^2(\lambda^4 + i\lambda^3 + \lambda^2 + i\lambda)}{2D(\omega^2 + \gamma^2)(1 + \lambda^2)}, \quad (56)$$

and $Q_f = Q/t_f$. Since, in the $t_f \rightarrow \infty$ limit, the exponent in the integrand in equation (55) is linear in t_f , the integral can be evaluated using the method of steepest descents [31]. In this method, the integral is approximated by the largest contribution that comes from the saddle point. The saddle point is determined by extremizing $S(\lambda)$. After finding out the saddle points, we deform the contour for λ in the complex plane in such a way that it passes through the saddle point and the saddle point corresponds to the maximum of $S(\lambda)$ along the path.

Since the derivative of $S(\lambda)$ with respect to λ is

$$S'(\lambda) = i\beta Q_f - \frac{\omega^2\eta^2}{2D(\omega^2 + \gamma^2)}(2\lambda + i), \quad (57)$$

there is only one saddle point λ_0

$$\lambda_0 = \frac{i(2\beta D Q_f(\omega^2 + \gamma^2) - \omega^2\eta^2)}{2\omega^2\eta^2} \quad (58)$$

located on the imaginary axis. We further note that there are two branch points located at $\pm i$, and we choose the imaginary axis extending from i to $+\infty$ and $-i$ to $-\infty$ to be the branch cut and the contour should not cross these cut lines. After doing a Taylor expansion and a Gaussian integral, we obtain the leading term of the heat distribution as

$$P(Q) \sim \frac{\beta}{2\pi} e^{-\frac{\eta^2}{2D\gamma}} \left(\frac{2\pi}{t_f |S''(\lambda_0)|} \right)^{1/2} \frac{\exp(t_f S(\lambda_0))}{(1 + \lambda_0^2)^{1/2}} e^{i\theta}. \quad (59)$$

where, double prime denotes two derivatives with respect to λ . θ gives the direction of the steepest descent and, in this case, it is given by

$$\theta = \frac{\pi}{2} - \frac{1}{2} \arg[S''(\lambda_0)] = 0 \quad (60)$$

which indicates a contour parallel to the real axis. In order to avoid crossing the branch cuts, we restrict Q_f such that the saddle point is always located between i and $-i$. The variation in the saddle point with Q for a given set of parameter values is shown in figure(3-a). Upon substituting λ_0 , $S(\lambda_0)$ and $|S''(\lambda_0)|$ into equation (59), the final form of the distribution, in the large time limit, becomes

$$P(Q) = \beta \left(\frac{D(\omega^2 + \gamma^2)}{2\pi t_f \omega^2 \eta^2} \right)^{1/2} \frac{e^{-\frac{\eta^2}{2D\gamma}}}{\left[1 - \frac{(2\beta D Q_f(\omega^2 + \gamma^2) - \omega^2 \eta^2)^2}{4\omega^4 \eta^4} \right]^{1/2}} \exp \left[\frac{-t_f (2\beta D Q_f(\omega^2 + \gamma^2) - \omega^2 \eta^2)^2}{8D\omega^2 \eta^2 (\omega^2 + \gamma^2)} \right]. \quad (61)$$

Since λ_0 must lie between $\pm i$, the Q_f -dependent part of the denominator of equation (61) can be approximated further and exponentiated to finally obtain a Gaussian distribution. Hence it appears that in the large time limit, the central part of the distribution is Gaussian and, as a consequence, the distribution satisfies the conventional fluctuation theorem for small fluctuations.

That the asymptotic result in the large time limit indicates a Gaussian behavior for small fluctuations is similar to what has been observed earlier through an explicit derivation of the heat distribution function for a uniformly moving parabolic potential [7, 9]. For large fluctuations, the distribution deviates from the Gaussian one. The existence of a non-Gaussian tail in the heat distribution for the same system has been also proved generally using the energy conservation relation[18]. Although, we have not evaluated an explicit analytical form of the distribution, under the most general circumstances, here also we expect similar non-Gaussian feature for large fluctuations. This inference is supported by results from numerical integration and simulations discussed below.

Next, we evaluate the integration in equation (54) numerically using MATLAB which implements adaptive Gauss-Kronrod quadrature formula. For the parameter values mentioned in figure(4-a), we perform the numerical integration

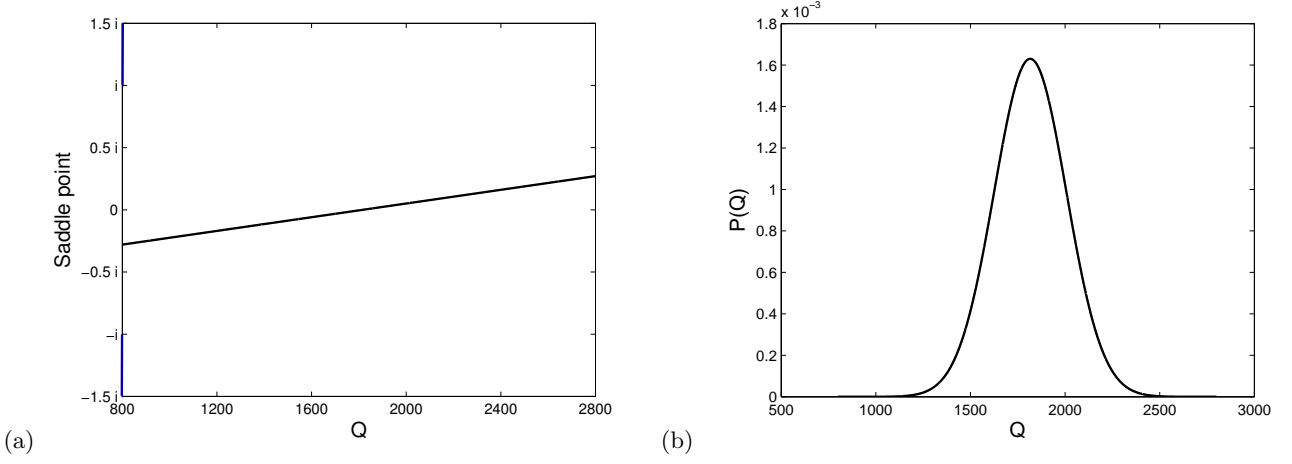


FIG. 3: (a) Plot of the saddle point with Q . We choose the range of Q such that the saddle point is in the range of $[-i : i]$. The bold blue lines above i and below $-i$ represent the branch cuts. The parameter values for this plot are $D = 0.05$, $\eta = 0.05$, $\omega = 0.1\pi$, $\gamma = 0.1$, $\beta = 0.1$, $\alpha = 200$ and $t_f = 8000$. (b) The asymptotic distribution of the dissipated heat at long time $t_f = 8000$ (see relation(61)). Other parameter values are same as those mentioned in (a).

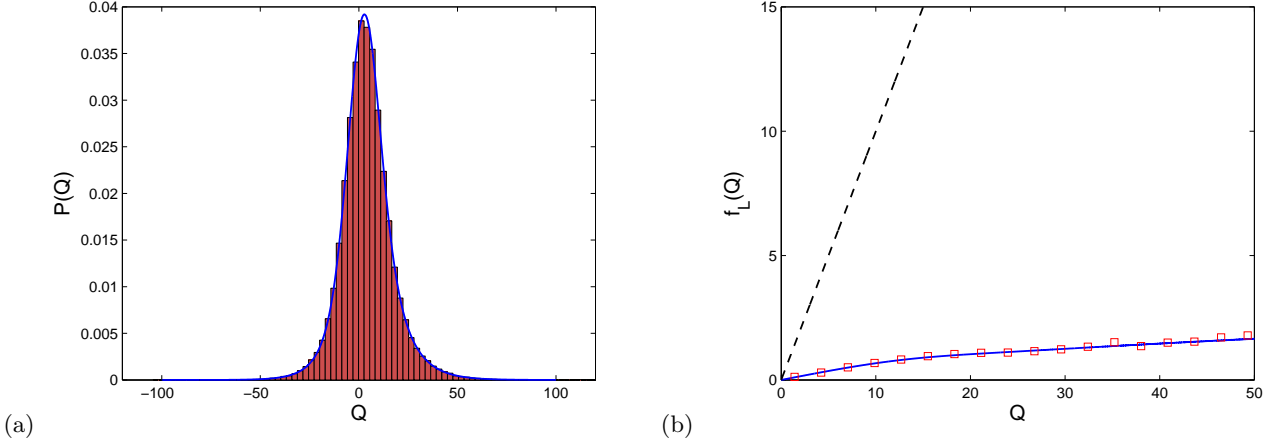


FIG. 4: (a) Distribution function of dissipated heat at time $t_f = 10$. The histogram is obtained from numerical simulations after averaging over 10^5 random trajectories. The solid blue line enveloping the histogram is obtained from the numerical integration of the expression appearing on r.h.s. of equation(54). Other parameter values are $D = 0.05$, $\eta = 0.05$, $\omega = 0.1\pi$, $\gamma = 0.1$, $\beta = 0.1$, $\alpha = 200$. (b) Plot of $\ln\left(\frac{P(Q)}{P(-Q)}\right)$ vs Q . The blue solid line is obtained from the numerical integration of the analytical expression (54), and the red squares are obtained from numerical simulations. The black dashed line is the prediction of the fluctuation theorem.

for which the error bound is 1.48×10^{-9} . The resulting distribution is plotted in figure(4-a) which also shows a reasonably good agreement with the histogram obtained from numerical simulations. Next, we consider the function $f_L(Q) = \ln\left(\frac{P(Q)}{P(-Q)}\right)$. To satisfy the transient fluctuation theorem, it is required that $f_L(Q) = Q$. In figure(4-b), we have plotted $f_L(Q)$ with Q for $t_f = 10$. From this plot, it is evident that the probability distribution function of the dissipated heat does not satisfy the transient fluctuation theorem.

VII. NUMERICAL SIMULATIONS

Using the Euler-Maruyama method [32], a discretized version of equation (2) can be written as

$$x_{n+1} = x_n - \Delta t \eta \cos(\omega n \Delta t) - \gamma x_n \Delta t + \sqrt{2D} d\xi_n, \quad (62)$$

where $\Delta t = (t_f - t_i)/N$ is a small time interval that divides the entire time interval $t_f - t_i$ into N parts and x_n denotes the position of the particle at $t_n = t_i + \Delta t n$ with $n = 0, 1, \dots, N$. $d\xi_1 \dots d\xi_n$ are independent normally distributed random variables with mean zero and standard deviation $\sqrt{\Delta t}$. These random variables are generated using the in-built ‘random’ function of MATLAB that supplies Gaussian-distributed random numbers $\mathcal{N}(0, 1)$ with zero mean and unit standard deviation.

After calculating the position of the particle at each time-step, we have calculated the work and dissipated heat at each time step using equation (22) and (47) respectively. To obtain the histogram for the work distribution, we have computed its values at final time $t_f = 1000$ for 40000 random trajectories with time step taken as $\Delta t = 0.05$. The histogram for the work probability distribution obtained from this data is shown in figure(1-a). The variations of the standard deviation with the strength and the angular frequency of the oscillatory drive are shown in figure (1-b) and (2-a), respectively. In figure (2-b), we have shown the variation of the central fourth moment $\langle (W - \langle W \rangle)^4 \rangle$ and the variance of the work distribution with η at large time $t_f = 1000$. The agreement with the relation $\langle (W - \langle W \rangle)^4 \rangle = 3(\langle W^2 \rangle - \langle W \rangle^2)^2$ is also shown in this figure. We have also seen the variation of the coefficient of skewness, $\frac{\langle (W - \langle W \rangle)^3 \rangle}{(\langle W^2 \rangle - \langle W \rangle^2)^{3/2}}$, with η . Over a range of η between $[0.05 : 1]$, the coefficient of skewness varies between 0.001 and 0.016.

To plot the distribution of dissipated heat, we compute the heat values at time $t_f = 10$ for 10^5 realizations with the time step $\Delta t = 0.0125$. The histogram is then compared with the analytical result in figure (4-a). In figure (4-b), we have compared the function $f_L(Q)$ obtained from numerical simulations with its values obtained after numerically evaluating the Fourier transform (54).

VIII. SUMMARY

In this paper, using the Onsager-Machlup fluctuation theory, we obtain the distribution functions for work and dissipated heat for a Brownian particle subjected to a confining harmonic potential and an oscillatory driving force. We start with a Langevin equation for the Brownian particle and obtain the transition probability in a functional integral form with an Onsager-Machlup type Lagrangian function. The final form of the transition probability is obtained by evaluating the contribution from the optimal path and deriving the functional integral explicitly for the fluctuations about the optimal path. From the Langevin equation and the energy conservation principle, we identify the total work done on the Brownian particle. This work consists of two parts, one associated with the change in the potential energy and the other, the heat dissipated to the reservoir. The Onsager-Machlup type Lagrangian function can be expressed in terms of the entropy production rate and the dissipation functions. The expressions for the entropy production rate and the work done by the external force, obtained above, are shown to be consistent with the energy conservation principle.

The expression for the total work is used further to define the work distribution function in a functional integral form. As before, the functional integral is evaluated by considering the optimal path and the fluctuations about this. The work distribution function satisfies the work fluctuation theorem in the long time limit. While the width of the distribution saturates for large values of the angular frequency of the oscillatory drive, the width increases with the angular frequency for small values of the frequency. Using the results derived in the work distribution part, we obtain the Fourier transform of the distribution of the dissipated heat. From this, using a saddle point approximation, an approximate analytical expression for the heat distribution is obtained in the long time limit. This result shows that for small fluctuations, the resulting distribution is Gaussian. The heat distribution, at finite time, is obtained by numerically evaluating the inverse Fourier transform. This result as well as the results from numerical simulations show that the heat distribution function does not satisfy transient fluctuation theorem.

Appendix A: Calculation of the functional integral

In this appendix we evaluate the functional integral of equation (15). The time interval is split into N slices through the following specifications $t_n = t_i + n\Delta t_N$ where $n = 1, 2, \dots, N$ and $\Delta t_N = (t_f - t_i)/N$. The functional integral can be written in the summation form as

$$\begin{aligned}
& \int \mathcal{D}z \exp \left[-\frac{1}{4D} \int_{t_i}^{t_f} dt [\gamma z_t + \dot{z}_t]^2 \right] \\
&= \lim_{N \rightarrow \infty} \left(\frac{1}{4\pi D \Delta t_N} \right)^{N/2} \int dz_{N-1} dz_{N-2} \dots dz_1 \exp \left[-\frac{1}{4D} \sum_{n=0}^{N-1} \Delta t_N \left(\frac{z_{n+1} - z_n}{\Delta t_N} + \gamma z_n \right)^2 \right] \\
&= \lim_{N \rightarrow \infty} \left(\frac{1}{4\pi D \Delta t_N} \right)^{N/2} \int dz_{N-1} dz_{N-2} \dots dz_1 \exp \left[-\frac{1}{4D \Delta t_N} \sum_{n=0}^{N-1} (z_{n+1} + z_n \phi)^2 \right], \tag{A1}
\end{aligned}$$

where $\phi = \Delta t_N \gamma - 1$. The Gaussian integral over all the z variables can be done using the matrix method. We however follow the straightforward method of completing square for one integral at a time. Starting with z_{N-1} integral, we have

$$\begin{aligned}
& \lim_{N \rightarrow \infty} \left(\frac{1}{4\pi D \Delta t_N} \right)^{N/2} \int dz_{N-1} dz_{N-2} \dots dz_1 \exp \left[-\frac{1}{4D \Delta t_N} \sum_{n=0}^{N-1} (z_{n+1} + z_n \phi)^2 \right] \\
&= \lim_{N \rightarrow \infty} \left(\frac{1}{4\pi D \Delta t_N} \right)^{(N-1)/2} (1 + \phi^2)^{-1/2} \int dz_{N-2} \dots dz_1 \exp \left[-\frac{1}{4D \Delta t_N} \sum_{n=0}^{N-3} (z_{n+1} + z_n \phi)^2 - \frac{1}{4D \Delta t_N} \frac{\phi^4}{1 + \phi^2} z_{N-2}^2 \right]. \tag{A2}
\end{aligned}$$

While doing this integration, we have used $z_N = 0$. After performing integrations over $N - 2$ variables starting with variable z_{N-1} , we are left with the final integration over z_1 . (A1) reduces to

$$\begin{aligned}
& \lim_{N \rightarrow \infty} \left(\frac{1}{4\pi D \Delta t_N} \right)^{N/2} \int dz_{N-1} dz_{N-2} \dots dz_1 \exp \left[-\frac{1}{4D \Delta t_N} \sum_{n=0}^{N-1} (z_{n+1} + z_n \phi)^2 \right] \\
&= \lim_{N \rightarrow \infty} \left(\frac{1}{4\pi D \Delta t_N} \right)^{-1} (1 + \phi^2 + \phi^4 + \dots + \phi^{2(N-2)})^{-1/2} \\
&\times \int dz_1 \exp \left[-\frac{1}{4D \Delta t_N} z_1^2 - \frac{1}{4D \Delta t_N} \frac{\phi^{2(N-1)}}{(1 + \phi^2 + \phi^4 + \dots + \phi^{2(N-2)})} z_1^2 \right]. \tag{A3}
\end{aligned}$$

The integration over z_1 leads to the final result

$$\begin{aligned}
& \lim_{N \rightarrow \infty} \left(\frac{1}{4\pi D \Delta t_N} \right)^{N/2} \int dz_{N-1} dz_{N-2} \dots dz_1 \exp \left[-\frac{1}{4D \Delta t_N} \sum_{n=0}^{N-1} (z_{n+1} + z_n \phi)^2 \right] \\
&= \lim_{N \rightarrow \infty} \left(\frac{1}{4\pi D \Delta t_N} \right)^{1/2} [1 + \phi^2 + \dots + \phi^{2(N-1)}]^{-1/2} \\
&= \lim_{N \rightarrow \infty} \left(\frac{2\pi D}{\gamma} \right)^{-1/2} \left(1 - \frac{\gamma(t_f - t_i)}{2N} \right)^{1/2} \left[1 - \left(1 - \frac{\gamma(t_f - t_i)}{N} \right)^{2N} \right]^{-1/2}. \tag{A4}
\end{aligned}$$

In order to obtain the last step, we have used

$$\left(1 + \phi^2 + \phi^4 + \dots + \phi^{2(N-1)} \right)^{-1/2} = \left[\frac{(1 - \phi^2)}{(1 - \phi^{2N})} \right]^{1/2}. \tag{A5}$$

Next, we need to consider $N \rightarrow \infty$ limit. This finally leads to

$$\int \mathcal{D}z \exp \left[-\frac{1}{4D} \int_{t_i}^{t_f} dt (\gamma z_t + \dot{z}_t)^2 \right] = \left(\frac{2\pi D}{\gamma} \right)^{-1/2} \left(1 - \exp[-2\gamma(t_f - t_i)] \right)^{-1/2}. \tag{A6}$$

Appendix B: Expressions appearing in the various integrations in section V and VI

The expressions for c_1 , c_2 and c_3 in equation(39) are

$$c_1 = \frac{2\gamma e^{2\gamma t_f}}{(e^{2\gamma t_f} - 1)}. \quad (\text{B1})$$

$$c_2 = -4\gamma \left[\frac{x_f \exp(\gamma t_f)}{(\exp(2\gamma t_f) - 1)} - A_W \right] e^{\gamma t_f} + \frac{2i\bar{\lambda}}{(\omega^2 + \gamma^2)} \bar{\omega} \quad (\text{B2})$$

and

$$\begin{aligned} c_3 = & -2\gamma \left[\frac{x_f \exp(\gamma t_f)}{\exp(2\gamma t_f) - 1} - A_W \right]^2 (1 - \exp(2\gamma t_f)) - \frac{\gamma \bar{\lambda}^2}{2(\omega^2 + \gamma^2)^2} + \frac{2i\bar{\lambda}\eta\gamma}{4\omega(\omega^2 + \gamma^2)} - \\ & \frac{2i\bar{\lambda}\omega}{(\omega^2 + \gamma^2)} \left[x_i + \frac{\eta\gamma}{(\omega^2 + \gamma^2)} \right] + \frac{\bar{\lambda}^2 t_f}{2(\omega^2 + \gamma^2)} + \frac{i\bar{\lambda}\eta\omega t_f}{(\omega^2 + \gamma^2)} - \frac{2i\bar{\lambda}\gamma}{(\omega^2 + \gamma^2)} \left[\frac{x_f \exp(\gamma t_f)}{\exp(2\gamma t_f) - 1} - A_W \right] \exp(\gamma t_f) \sin \omega t_f - \\ & \left[\frac{\bar{\lambda}^2(\omega^2 - \gamma^2)}{4\omega(\omega^2 + \gamma^2)^2} + \frac{2i\bar{\lambda}(\eta\omega - i\bar{\lambda})}{4\omega(\omega^2 + \gamma^2)} \right] \sin 2\omega t_f + \frac{2i\bar{\lambda}\omega \exp(-\gamma t_f)}{(\omega^2 + \gamma^2)} \left[x_i + \frac{\eta\gamma}{(\omega^2 + \gamma^2)} + \frac{x_f \exp(\gamma t_f)}{(\exp(2\gamma t_f) - 1)} - A_W \right] \\ & - \frac{2i\bar{\lambda}\omega}{(\omega^2 + \gamma^2)} \exp(\gamma t_f) \left[\frac{x_f \exp(\gamma t_f)}{(\exp(2\gamma t_f) - 1)} - A_W \right] \cos \omega t_f + \frac{1}{4\omega} \left[\frac{2\gamma\omega\bar{\lambda}^2}{(\omega^2 + \gamma^2)^2} - \frac{2i\bar{\lambda}\eta\gamma}{(\omega^2 + \gamma^2)} \right] \cos 2\omega t_f, \end{aligned} \quad (\text{B3})$$

where $\bar{\omega} = \omega \cos \omega t_f + \gamma \sin \omega t_f$.

The expressions for m_1 and m_2 in equation (41) of the main text are

$$\begin{aligned} m_2 = & -[\gamma^2\omega(1 + e^{2\gamma t_f}) + \omega^3(1 - e^{2\gamma t_f}) - 2e^{2\gamma t_f}\gamma\omega t_f(\gamma^2 + \omega^2) - \gamma^2\omega \cos(2\omega t_f)(1 + e^{2\gamma t_f}) \\ & + \omega^3 \cos(2\omega t_f)(1 - e^{2\gamma t_f}) + 2\gamma\omega^2 \sin(2\omega t_f) + e^{2\gamma t_f}\gamma(\gamma^2 + \omega^2) \sin(2\omega t_f)](16De^{2\gamma t_f}\gamma\omega(\gamma^2 + \omega^2)^2)^{-1} \end{aligned} \quad (\text{B4})$$

and

$$m_1 = -\frac{i}{8} \left[\eta\gamma(\cos 2\omega t_f - 1) + (x_i + \frac{\eta\gamma}{(\omega^2 + \gamma^2)})4\omega(\omega - \bar{\omega} \exp[-\gamma t_f]) - 2\omega^2\eta t_f + \eta\omega \sin 2\omega t_f \right] (D\omega(\gamma^2 + \omega^2))^{-1} \quad (\text{B5})$$

The expressions for l_4, l_3, l_2, l_1, l_0 appearing in equation(53) are,

$$\begin{aligned} l_4 = & -2\eta^2\gamma\omega \left\{ (1 + e^{2\gamma t_f})\gamma\omega \cos(2\omega t_f) + e^{\gamma t_f} \left[-2\gamma\omega \cosh(\gamma t_f) + 2\omega t_f \sinh(\gamma t_f)(\omega^2 + \gamma^2) \right. \right. \\ & \left. \left. + (\omega^2 - \gamma^2) \sin(2\omega t_f) \sinh(\gamma t_f) \right] \right\}. \end{aligned} \quad (\text{B6})$$

$$\begin{aligned} l_3 = & -2\eta^2\gamma\omega \left\{ (1 + e^{2\gamma t_f})\gamma\omega \cos(2\omega t_f) + e^{\gamma t_f} \left[-2\gamma\omega \cosh(\gamma t_f) + 2\omega t_f \sinh(\gamma t_f)(\omega^2 + \gamma^2) \right. \right. \\ & \left. \left. + (\omega^2 - \gamma^2) \sin(2\omega t_f) \sinh(\gamma t_f) \right] \right\}. \end{aligned} \quad (\text{B7})$$

$$\begin{aligned} l_2 = & \eta^2\gamma \left\{ -2\gamma(\gamma^2 + 2\omega^2) + 8e^{\gamma t_f}\omega^3 \sin(\omega t_f) + e^{2\gamma t_f} \left[2\gamma(\gamma^2 + 3\omega^2) - 2\omega^2(\omega^2 + \gamma^2)t_f \right. \right. \\ & \left. \left. - 2\gamma\omega^2 \cos(2\omega t_f) + (\gamma^2 - \omega^2)\omega \sin(2\omega t_f) \right] \right\}. \end{aligned} \quad (\text{B8})$$

$$\begin{aligned} l_1 = & \eta^2\omega \left\{ 2\omega^3 + 8e^{\gamma t_f}\gamma\omega^2 \sin(\omega t_f) - e^{2\gamma t_f} \left[-2\omega\gamma^2 + 2\omega^3 + 2\omega\gamma t_f(\omega^2 + \gamma^2) \right. \right. \\ & \left. \left. + 2\omega\gamma^2 \cos(2\omega t_f) + \gamma(\omega^2 - \gamma^2) \sin(2\omega t_f) \right] \right\}. \end{aligned} \quad (\text{B9})$$

and

$$l_0 = 2e^{2\gamma t_f} \eta^2 (\omega^2 + \gamma^2)^2. \quad (\text{B10})$$

-
- [1] L. E. Reichl, *A modern course in Statistical Physics* (Wiley-VCH, Weinheim, 2013).
- [2] R. Kubo, Rep. Prog. Phys. **29**, 255 (1966).
- [3] D. J. Evans, E. G. D. Cohen and G. P. Morriss, Phys. Rev. Lett. **71**, 2401 (1993); D. J. Evans and D. J. Searles, Phys. Rev. E **50**, 1645 (1994).
- [4] G. Gallavotti and E. G. D. Cohen, Phys. Rev. Lett. **74**, 2694 (1995); J. Stat. Phys. **80**, 931 (1995).
- [5] J. Kurchan, J. Phys. A : Math. Gen. **31**, 3719 (1998).
- [6] J. L. Lebowitz and H. Spohn, J. Stat. Phys. **95**, 333 (1999).
- [7] R. van Zon and E. G. D. Cohen, Phys. Rev. Lett. **91**, 110601 (2003).
- [8] R. van Zon and E. G. D. Cohen, Phys. Rev. E **67**, 046102 (2003).
- [9] R. van Zon and E. G. D. Cohen, Phys. Rev. E **69**, 056121 (2004).
- [10] U. Seifert, Phys. Rev. Lett. **95**, 040602 (2005); U. Seifert, Eur. Phys. J. B **64**, 423 (2008).
- [11] R. J. Harris and G. M. Schütz, J. Stat. Mech. P07020 (2007).
- [12] L. Onsager and S. Machlup, Phys. Rev. **91**, 1505 (1953).
- [13] S. Machlup and L. Onsager, Phys. Rev. **91**, 1512 (1953).
- [14] L. Onsager Phys. Rev. **37**, 405 (1931); L. Onsager, Phys. Rev. **38**, 2265 (1931).
- [15] L. Bertini, A. De Sole, D. Gabrielli, G. Jona-Lasinio, and C. Landim, Phys. Rev. Lett. **87**, 040601 (2001) .
- [16] L. Bertini, A. De Sole, D. Gabrielli, G. Jona-Lasinio, and C. Landim, J. Stat. Phys. **107**, 635 (2002).
- [17] L. Bertini, A. De Sole, D. Gabrielli, G. Jona-Lasinio, and C. Landim, J. Stat. Phys. **123**, 237 (2006).
- [18] T. Taniguchi and E. G. D. Cohen, J. Stat. Phys. **126** 1 (2007).
- [19] T. Taniguchi and E. G. D. Cohen, J. Stat. Phys. **130**, 1 (2008); T. Taniguchi and E. G. D. Cohen, J. Stat. Phys. **130**, 633 (2008).
- [20] E. G. D. Cohen, J. Stat. Mech. P07014 (2008).
- [21] C. Maes, K. Netočný and B. Wynants, J. Phys. A: Math. Theor. **42**, 365002 (2009) .
- [22] A. Engel, Phys. Rev. E **80**, 021120 (2009); D. Nickelsen and A. Engel, Eur. Phys. J B **82**, 207 (2011).
- [23] T. Speck and U. Seifert, Eur. Phys. J. B **43**, 521 (2005).
- [24] A. Imparato, L. Peliti, G. Pesce, G. Rusciano and A. Sasso, Phys. Rev. E **76**, 050101(R) (2007) .
- [25] N. Singh, J. Stat. Phys. **131**, 405 (2008).
- [26] H. Risken, *The Fokker-Planck Equation : Methods of Solution and Applications* (Springer-Verlag, Berlin,1989).
- [27] F. W. Wiegul, *Introduction to Path Integral Methods in Physics and Polymer Science* (World Scientific, Singapore, 1986).
- [28] For a linear model, an approximation through most probable path is expected to be a good approximation in the small D limit [27].
- [29] K. Sekimoto, Prog. Theor. Phys. Supp. **130**, 17 (1998).
- [30] O. Mazonka and C. Jarzynski, arXiv:cond-mat/9912121 (1999).
- [31] G. B. Arfken and H. J. Weber, *Mathematical Methods for Physicists*, 6th ed. (Elsevier, Boston,MA,2005).
- [32] D. Higham, SIAM Review **43**, 525 (2001).